Dissociative adsorption of H2 on Cu(100): A four-dimensional study of the effect of rotational motion on the reaction dynamics.

Mowrey, R.C.; Kroes, G.J.; Wiesenekker, G.; Baerends, E.J.

published in
Journal of Chemical Physics
1997

DOI (link to publisher)
10.1063/1.473515

document version
Publisher's PDF, also known as Version of record

Dissociative adsorption of H_2 on Cu(100): A four-dimensional study of the effect of rotational motion on the reaction dynamics

R. C. Mowrey
Theoretical Chemistry Section, Code 6179, Naval Research Laboratory, Washington, DC 20375-5342

G. J. Kroes
LIC, Gorlaeus Laboratoria, Rijksuniversiteit Leiden, Postbus 9502, 2300 RA Leiden, The Netherlands

G. Wiesenekker and E. J. Baerends
Theoretische Chemie, Vrije Universiteit, De Boelelaan 1083, 1081 HV Amsterdam, The Netherlands

(Received 30 September 1996; accepted 9 December 1996)

The reaction of H_2 on Cu(100) is investigated using a four-dimensional (4D) quantum dynamical fixed-site model to assess the influence of molecular rotation on dissociation over the most reactive (the bridge) site. The potential energy surface (PES) is a fit to the results of density functional calculations performed using a generalized gradient approximation treating a Cu slab with a periodic overlayer of H_2. Dissociation probabilities for molecules with ''helicoptering'' ($m_j=j$) and ''cartwheeling'' ($m_j=0$) rotational motions are here found to be comparable because of the strong corrugation in the azimuthal coordinate. The calculations indicate that reaction is accompanied by significant rotationally inelastic scattering. Surprisingly, vibrational excitation is also found to be an efficient process in collisions with the reactive bridge site. In these collisions, the molecular axis is tilted away from the orientation parallel from the surface. Considering the approximate nature of the 4D model used, the calculated reaction probabilities are in good agreement with experiment, indicating that the PES that was used is accurate. © *1997 American Institute of Physics.* [S0021-9606(97)03510-1]

I. INTRODUCTION

Activated dissociation of H_2 on copper surfaces is one of the most studied subjects in the area of gas–surface reaction dynamics. The results of experiments measuring the dependence of the dissociation probability on the incidence angle, translational energy, and the rovibrational state of the molecule[1–13] are available as benchmarks to which the results of computational models[14–38] can be compared. To date, a full six-dimensional (6D) quantum mechanical description of activated dissociation of H_2 has not yet been carried out but low-dimensional models treating the most important coordinates have successfully explained many experimental observations. Two-dimensional (2D) models demonstrated that vibrational energy increases the reactivity for systems where the dissociation barrier lies in the products channel.[14–19] The importance of rotational motion was demonstrated in three-dimensional (3D) and four-dimensional (4D) calculations, which showed that important dynamical effects are lost in calculations that restrict the molecular orientation.[19–30] The role of translational motion parallel to the surface has been studied using other computational models.[31–38]

In the current study we use a 4D model in which the H_2 center of mass remains fixed over a bridge site on the Cu(100) surface. Dissociation above this site (with the atoms moving to the hollow sites) has the lowest associated dissociation barrier of all the high-symmetry impact sites. It is reasonable to expect this configuration and those closely related to it to be the most important contributors to dissociation near the energetic threshold. The model treats the surface atoms as static and the scattering occurs on a single potential energy surface. The model incorporates important aspects of the surface corrugation because the H_2–surface interaction depends on the azimuthal angle of the molecular axis: the $\phi=0°$ and $\phi=90°$ ($\theta=90°$) orientations show both the lowest (0.48 eV) and the highest (1.37 eV) barriers that are associated with the four dissociation routes investigated previously for parallel approaches of the molecule.[39] Similar models have been used to study dissociation on the Cu(111) surface.[28,30] Center-of-mass motion normal to the surface, the H–H internuclear separation, and the coordinates defining the orientation of the molecular axis are explicitly included in the calculation and are treated quantum mechanically. The time-dependent Schrödinger equation is solved using a wave-packet method. Although the model does not provide quantitative agreement with experimental observations, the calculations yield important new insights into the dynamics of the reaction and rovibrationally inelastic scattering from the bridge site.

An important element in the present work is the use of a potential energy surface (PES), which is a fit to recent electronic structure calculations.[39] Density functional theory (DFT) incorporating a generalized gradient approximation was used to determine the energetics of an overlayer of hydrogen molecules above a copper slab for a large number of molecular geometries. The results of these calculations were fit to analytic functions to provide 2D, 4D, and 6D PESs for the H_2+Cu(100) system. Previous studies have used these potentials in a 2D model for dissociation above a bridge site to hollow sites[18] and in a 4D model examining the influence of the variation of the barrier height with the surface impact

 0021-9606/97/106(10)/4248/12/$10.00

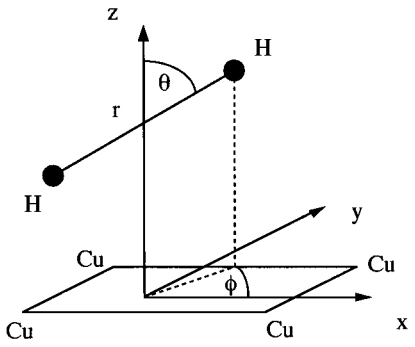

FIG. 1. Coordinate system used in 4D H_2/Cu(100) calculations.

point and the influence of the availability of diffraction channels.[37,38] The present work complements these studies by focusing on the effects of rotational motion on the dissociation dynamics.

The computational model, including an outline of the wave-packet method and a description of the PES, used, are described in Sec. II. The results of the 4D calculations and discussion are given in Sec. III. We also describe some 2D calculations in which the rotational angle is held fixed, which aid in interpreting some of the 4D results. Sec. IV presents the conclusions drawn from the work.

II. THEORY

The model problem considered here is for dissociation of H_2 above a Cu–Cu bridge site on the (100) surface. The coordinate system used is illustrated in Fig. 1. In the present calculations, X and Y are kept fixed so that the molecular center of mass is constrained to remain above the bridge site. The dynamics of the Cu atoms are not treated in the model. The Hamiltonian describing the motion of the H nuclei is given by

$$\hat{H}=-\frac{\hbar^2}{2M}\frac{\partial^2}{\partial Z^2}-\frac{\hbar^2}{2\mu}\frac{\partial^2}{\partial r^2}+\frac{\hat{j}^2}{2\mu r^2}+V_{4D}(Z,r,\theta,\phi), \quad (1)$$

where M and μ are the total mass and reduced mass of H_2, respectively, $\hat{j}^2$ is the square of the rotational angular momentum operator, and V_{4D} is the interaction potential.

The interaction potential is represented by the expression

$$\begin{aligned}V_{4D}(Z,r,\theta,\phi)&=V_{00b}(Z,r)Y_{00}(\theta,\phi)\\&+V_{20b}(Z,r)Y_{20}(\theta,\phi)\\&+V_{20e}(Z,r)Y_{2e}(\theta,\phi),\end{aligned} \quad (2)$$

where Y_{00} and Y_{20} are spherical harmonic functions and Y_{2e} is given by

$$Y_{2e}(\theta,\phi)=\sqrt{\tfrac{1}{2}}[Y_{22}(\theta,\phi)+Y_{2-2}(\theta,\phi)]. \quad (3)$$

The expansion coefficients are related to four 2D potential energy surfaces fitted to the results of density functional calculations. These 2D potentials describe dissociation with parallel (θ=90°) and tilted (θ=140.8°) orientations toward the hollow (ϕ=0°) and top (ϕ=90°) surface sites. The DFT calculations were performed using the generalized gradient approximation. Complete details of the DFT calculations and fitting procedure are available in Ref. 39. The barrier for dissociation to hollow sites is located at $Z=1.99a_0$ and $r=2.33a_0$ with a height of 0.48 eV. Dissociation to top sites is endothermic with a barrier of 1.37 eV located at $Z=2.86a_0$ and $r=3.95a_0$.

The wave function is represented using the close-coupling wave-packet, (CCWP) method,[40–42] which combines a description of the rotational degrees of freedom using an expansion in a set of spherical harmonic basis functions with a grid representation of motion in the Z and r coordinates. Large basis expansions were needed for these calculations since the energy of the rotational states decreases as r increases. As the molecule dissociates, states with large values of j become energetically accessible and must be included in the expansion. For example, the energy of the $j=20$ state is approximately 1 eV for $r=2.5a_0$. Numerical tests indicated that converged results were obtained by including states up to $j=28$. While, for large expansions, the computational work in the CCWP method may scale as the square of the number of basis functions, it is often possible to exploit the sparseness of the potential coupling matrix to obtain a more favorable scaling.[43,44] In this particular case, the interaction potential used is such that it couples spherical harmonic functions that differ only by Δj, $\Delta m_j=0, \pm 2$. Although 225 basis functions were included for calculations for even j, each rotational state is coupled to at most nine other states so the computational work associated with the potential term in the Hamiltonian scales as $\sim 225\times 9$ instead of 225^2.

The size of the two-dimensional grids describing the Z and r dependence of the wave function is reduced by using L-shaped grids that cover the regions of coordinate space where the wave function is nonzero.[45] A total of 192 and 32 grid points were used in the Z coordinate in the reactants–interaction and products regions, respectively. In the r coordinate 16 grid points were used in the reactants–interaction region and an additional 16 points were added in the products regions. The grid extended from $Z=-1.0a_0$ to $Z=27.65a_0$ and from $r=0.4a_0$ to $r=6.6a_0$.

For the Hamiltonian given above the time-dependent Schrödinger equation can be written as an initial value problem. The initial wave function representing the incident H_2 in a state with rotational quantum numbers j_0 and m_{j0} and vibrational quantum number ν_0, and with a distribution of values of center-of-mass translational momentum is written as

$$\begin{aligned}&\Psi(Z,r,\theta,\phi,t=0)\\&=Y_{j_0m_{j_0}}(\theta,\phi)\chi_{\nu_0j_0}(r)\int_{-\infty}^{\infty}dk_z b(k_z)\frac{\exp(ik_zZ)}{\sqrt{2\pi}},\end{aligned} \quad (4)$$

where $\chi_{\nu_0j_0}$ is the vibrational wave function. The momentum distribution has a Gaussian form in these calculations and is given by

$$b(k_z)=\left(\frac{2\zeta^2}{\pi}\right)^{1/4}\exp[-(k_{z_0}-k_z)^2\zeta^2+i(k_{z_0}-k_z)Z_0]. \tag{5}$$

The wave function has a width ζ, and is centered on the point Z_0, having an average translational momentum of k_{z_0}. For each initial rovibrational state of interest, calculations were performed for two different energy ranges. Low-energy collisions of H_2 in the ground rovibrational state were studied using the parameters $\zeta=0.5364a_0$ and $k_{z_0}=10.87a_0^{-1}$ and for higher collision energies $\zeta=0.5222a_0$ and $k_{z_0}=14.10a_0^{-1}$ were used. These k_{z_0} values correspond to total energies of 0.696 and 0.995 eV, respectively. For other initial rotational states the value of k_{z_0} was adjusted so that the most probable total energy was the same as that of the ground rovibrational state. The initial wave function was centered at $Z_0=17.0a_0$ in all calculations.

The value of Ψ at later times is evaluated by computing the action of the time evolution operator on the initial wave function. This is done by expanding the evolution operator in a series of Chebyshev polynomials.[46] Implementation of this method involves the repeated application of the Hamiltonian operator to the wave function. Within the CCWP representation, the rotational term in the Hamiltonian is a local operator that is evaluated by multiplying the wave function by the appropriate eigenvalue. The potential energy term is local in r and Z and nonlocal in j and m_j, involving sparse-matrix vector multiplications on the grid points in r and Z. The terms representing the center-of-mass translational energy and vibration are nonlocal and are evaluated using the fast Fourier transform method.[47,48] Time steps of 100 a.u. were used in the calculations.

S-matrix elements describing transitions between the initial state of the wave function and final scattered gas-phase states are computed using a procedure developed by Balint–Kurti and co-workers[49–51] to treat photodissociation and collinear atom–diatom scattering. More recently, the method was extended to treat diatom–surface scattering.[52] A dividing surface defined by $Z=Z_\infty$ is selected in the asymptotic gas-phase region where the interaction between the molecule and the surface is negligible and the amplitude of the incident wave function is zero. As the wave function is propagated in time, the overlap of the wave function with the eigenstates of the gas-phase molecule at the dividing surface are computed at regular time intervals

$$C_{j'm_j'\nu'}(Z_\infty,t)=\int dr\,\chi^*_{\nu'j'}(r)\int d\hat{\mathbf{r}}Y^*_{j'm_j'}(\hat{\mathbf{r}})\Psi(Z_\infty,r,\hat{\mathbf{r}},t), \tag{6}$$

where $\hat{\mathbf{r}}=(\theta,\phi)$. These time-dependent coefficients are transformed into energy-resolved coefficients by use of half-Fourier transforms

$$A_{j'm_j'\nu'}(E')=\int_0^{t'}dt e^{iE't/\hbar}C_{j'm_j'\nu'}(Z_\infty,t), \tag{7}$$

where E' is the total energy of the molecule. The integration over time continues as long as the wave packet continues to have amplitude at the analysis surface. The energy-resolved coefficients can be evaluated over the range of energies for which the incident wave packet has nonnegligible amplitude. The S-matrix elements are given by

$$S_{j_0m_{j0}\nu_0\to j'm_j'\nu'}(E')=\delta_{j_0j'}\delta_{m_{j0}m_j'}\delta_{\nu_0\nu'}e^{-i2k_z'Z_\infty}-\left(\frac{k_z'k_{j'\nu'}'}{2\pi}\right)^{1/2}\frac{\hbar e^{-ik_{j'\nu'}'Z_\infty}}{Mb(-k_z')}A_{j'm_j'\nu'}(E'), \tag{8}$$

where $k'_{j'\nu'}=[2M(E'-\epsilon_{j'\nu'})/\hbar^2]^{1/2}$ and $k_z'=[2M(E'-\epsilon_{j_0\nu_0})/\hbar^2]^{1/2}$. Since the probability of a transition between the initial state and each final gas-phase rovibrational state is given by the squared modulus of the S-matrix element, the dissociation probability, P_D, for an incident energy E' is given by

$$P_D=1-\sum_{j'm_j'\nu'}|S_{j_0m_{j0}\nu_0\to j'm_j'\nu'}(E')|^2. \tag{9}$$

The summation includes all energetically accessible gas-phase states at the energy of interest.

Since the scattering information is obtained by analyzing the outgoing wave function at $Z=Z_\infty$, the outgoing wave function is not needed beyond this point and can be removed using an optical potential. The functional form used is[53]

$$V_{\rm abs}(x)=\begin{cases} iV^{\rm abs}_{\rm max}[(x-x^{\rm abs}_{\rm min})/(x^{\rm abs}_{\rm max}-x^{\rm abs}_{\rm min})]^2, & x^{\rm abs}_{\rm min}\leqslant x\leqslant x^{\rm abs}_{\rm max},\\ 0, & x<x^{\rm abs}_{\rm min},\end{cases} \tag{10}$$

where the variable x is Z and r in the reactants and products asymptotic regions, respectively. The final state analysis was performed at $Z_\infty=20.75a_0$. The parameters for the absorbing potential in the gas-phase region were $Z^{\rm abs}_{\rm min}=21.05a_0$ and $Z^{\rm abs}_{\rm max}=27.65a_0$. For the absorbing potential on the surface, the values $r^{\rm abs}_{\rm min}=4.8a_0$ and $r^{\rm abs}_{\rm max}=6.6a_0$ were used. The strength, $V^{\rm abs}_{\rm max}$, of the absorbing potentials was 1.0 eV.

III. RESULTS AND DISCUSSION

Dissociation probabilities and probabilities for transitions to final gas-phase states were computed for various initial rovibrational states of H_2. Figure 2 shows the probabilities for dissociation of H_2 initially in the ground rovibrational state as a function of incident translational energy. The dissociation probability becomes nonzero when the translational energy reaches 0.37 eV and increases rapidly with increasing energy. The curve exhibits a number of maxima and minima that are mostly related to the opening up of additional channels.[54,55] The dissociation probability reaches a maximum value of 0.46 but then decreases to an asymptotic value of about 0.4. The dynamical threshold, defined as the energy at which the probability is half its asymptotic value, is at 0.47 eV. This value corresponds closely to the

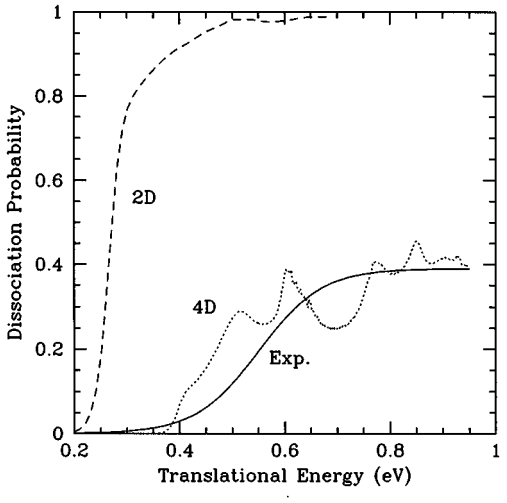

FIG. 2. Computed dissociation probability of H_2 as a function of translational energy for the $\nu_0=0$, $j_0=0$ state. The dissociation probability from a 2D model (Ref. 18) and a fit to experimental measurements (Ref. 57) are shown.

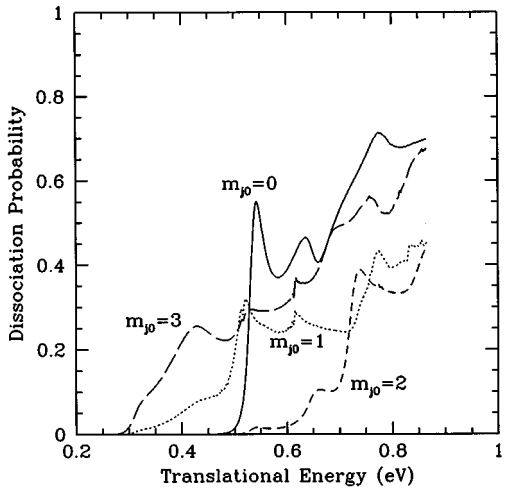

FIG. 3. Dissociation probability of H_2 as a function of translational energy for the $\nu_0=0$, $j_0=3$ states.

barrier height of 0.48 eV from the PES. Other computational studies have found similar correspondence between the dynamical threshold and the height of the effective barrier.[26,56] The dynamical threshold may be seen as an effective barrier height, i.e., as the sum of the potential barrier height and the difference of the zero-point energy of the molecule at the transition state and of the molecule in the gas phase. The close correspondence between the computed threshold value and the barrier height of the PES suggests that the zero-point energy at the barrier is comparable to that of gas-phase H_2.

The results of earlier calculations[18] using a 2D model with the same potential used here but with θ and ϕ fixed at 90° and 0°, respectively, are reproduced in Fig. 2. The 2D results have a lower dynamical threshold than the 4D results, illustrating that dissociation occurs most readily when the molecule is parallel to the surface with its internuclear bond pointed toward the surface hollow sites. The lower saturation value seen in the 4D calculations is due to collisions being unreactive for many molecular orientations. As will be discussed later on, 2D calculations show that orientations in which $\theta=90°$ and the atoms point to the top sites are unreactive. Likewise, the 2D calculations suggest that reaction does not occur for any angle ϕ for angles θ that differ from 90° by more than 20°.

The dissociation probability for H_2 initially in the ground vibrational state obtained from a fit to experimental measurements is shown in Fig. 2.[57] Experimental measurements were fit to the functional form

$$P_\nu(E)=\frac{A}{2}\,(1+\tanh\{[E-T(\nu)]/W(\nu)\}), \tag{11}$$

where ν is the initial vibrational state of the molecule, A is the saturation value, T is the energetic threshold, and W is the width of the dissociation probability versus energy curve. The computed saturation value, 0.40, and the experimental value, 0.39, are in good agreement. The computed dynamical threshold, 0.47 eV, is about 0.1 eV lower than the experimental value of 0.58 eV.[57] It is likely that the difference is due, in part, to the neglect of parallel translational motion. Previous 4D calculations in which the H_2 orientation was kept fixed but in which barriers across the whole unit cell were sampled[37,38] showed that, compared to the 2D bridge-to-hollow model, the dynamical threshold associated with the reaction probability increases by 0.2 eV when parallel translational motion is included. A definite verdict on the accuracy of the PES has to await 6D calculations modeling all molecular degrees of freedom. It is encouraging that the present 4D result comes out 0.1 eV too low rather than too high.

The dependence of the dissociation probability on incident translational energy for molecules initially in the $j_0=3$ and 4 states is shown in Figs. 3 and 4, respectively. Figures 3 and 4 show that the probability is strongly dependent on the m_j quantum number. In particular, initial quantum states

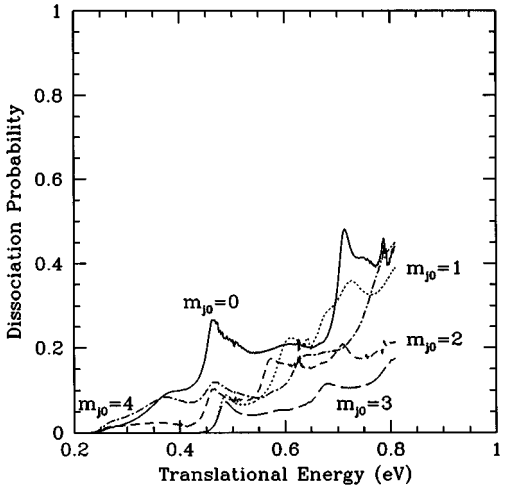

FIG. 4. Dissociation probability of H_2 as a function of translational energy for the $\nu_0=0$, $j_0=4$ states.

with $j_0+m_{j_0}$ equal to an even integer have lower thresholds for dissociation than those with $j_0+m_{j_0}$ odd. Sheng and Zhang[23] previously found this result in calculations using a flat surface model. The wave function describing the incident molecule in the rotational state j_0, m_{j_0} is an eigenfunction of the exchange operator with eigenvalue $(-1)^{j_0}$. The wave function describing the dissociated atoms on the surface is also an eigenfunction of the exchange operator and has the eigenvalue $(-1)^{m_{j_0}}$ for symmetric molecule–surface vibrational states (which includes the ground state) and either $+(-1)^{m_{j_0}}$ or $-(-1)^{m_{j_0}}$ for antisymmetric molecule–surface vibrational states. During the collision with the flat surface, the azimuthal quantum number is conserved. This gives rise to the restriction that for states with $j_0+m_{j_0}$ odd the antisymmetric molecule–surface stretch mode is always excited with at least one quantum, both at the transition state and in the atom–surface potential energy minimum.[23] The reason that we obtain the same result here is a consequence of the twofold rotational symmetry of the fixed-site model; the PES for such a model allows transitions in the m_j quantum number but only by even integers so the eigenvalues of the exchange operator remain the same as for the flat surface model. The same result would, of course, be obtained for any fixed-site model of $2n$-fold rotational symmetry.

An unexpected result regarding the dependence of the dissociation probability on the initial m_j quantum number is that molecules rotating in a cartwheel fashion $(m_{j_0}=0)$ are nearly as likely to dissociate as those rotating like helicopters $(m_{j_0}=j)$. This behavior differs from that seen in other calculations of scattering from flat[23,25] and corrugated[28,30] surfaces, which predict that molecules rotating with a helicopter-type motion are more likely to dissociate than those with a cartwheel-type motion. For instance, the dissociation threshold of the $j=5$ manifold was found to show a monotonic decrease as m_j increased from 0 to 5 in a recent computational study of the H_2/Cu(111) system that used a potential with azimuthal corrugation.[30] The preference for dissociation of helicopter-type motion was explained as arising from the fact that dissociation occurs only when the molecular bond is nearly parallel to the surface. Since helicoptering molecules spend a greater fraction of their time with the preferred orientation than cartwheeling molecules, they would then have larger dissociation probabilities:

The present calculations indicate that the situation can be more complicated for surfaces with strong azimuthal corrugation. For dissociation above a bridge site, the minimum energy dissociation pathway occurs with the internuclear axis lying parallel to the surface ($\theta=90°$) and pointing toward the fourfold hollow sites ($\phi=0°$). The wave function representing the dissociated atoms will have a large amplitude above the hollow sites but will be negligible above the top sites ($\phi=90°$) because the barrier for dissociation to the top sites is very high (1.37 eV).[39] An incident wave function with this same symmetry would be expected to have the largest possible dissociation probabilities. For example, an incident wave function containing equal contributions of the Y_{11} and Y_{1-1} rotational states might be optimal for dissociation because its highest probability occurs for $\theta=90°$, $\phi=0°$ while for $\phi=90°$ the probability is zero.

Considering incident molecules with helicopter-type motion, although their angular distribution is largest for θ near 90°, the azimuthal distribution is isotropic, as it is for all values of m_j, rather than centered around $\phi=0°$, which would be optimal. Incident molecules with cartwheeling motion will not have the proper orientation in either θ or ϕ to dissociate readily. For both helicoptering and cartwheeling rotational motion, dissociation can occur if the PES induces transitions to other rotational states to produce, by superposition, a wave function describing a properly oriented molecule at the transition state. Focusing on the azimuthal orientation, if the proper wave function contains equal contributions of $+m_j$ and $-m_j$ quantum states for each j (as is the case for the ''optimal'' $Y_{1,1}+Y_{1-1}$ state), this is achieved most easily for cartwheeling motion because the symmetry of the surface is such that the $m_{j_0}=0$ state is coupled equally well to the $+m_j$ and $-m_j$ states for a particular j state. For helicoptering motion, populating the $-m_j$ state when the azimuthal quantum number of the incident molecule is $+m_j$ requires a large Δm_j if j is very large. For either case, it is likely that formation of a wave function with the proper symmetry in θ and ϕ at the transition state will require populating rotational states with significantly different values m_j and, perhaps, j quantum numbers than those of the incident wave function. Recent experimental observations of the rotational distributions of D_2, which associatively desorbs from Cu(111), indicate that dissociation probabilities of molecules with helicopter and cartwheel rotational motion may be comparable,[58] and that the preference for dissociation of molecules with helicopter-type rotation is not as high as suggested by previous model calculations.[25,27,28,30] The strong preference for helicopter dissociation found in these studies was either due to the use of a flat surface model[25,27] or due to the use of a potential that did not incorporate the ϕ dependence as rigorously as our potential.[39] Furthermore, all these calculations dealt with the less-corrugated (111) surface of copper.

As was seen for the ground rovibrational state, there is a significant amount of structure evident in the dissociation probabilities in Figs. 3 and 4. Some features such as the location of broad maxima are common to several of the initial states and seem to be related to new channels opening up.[54,55] For example, the maximum in the $j=0$ curve in Fig. 2 at $E=0.6$ eV occurs at the same total energy as the maxima in the $j_0=3$, $m_{j_0}=1$ and $j_0=3$, $m_{j_0}=3$ curves at $E=0.53$ eV and the $j_0=4$, $m_{j_0}=0$, $j_0=4$, $m_{j_0}=2$, and $j_0=4$, $m_{j_0}=4$ curves at $E=0.47$ eV. Other features such as the spike at $E=0.63$ eV in the $j_0=4$, $m_{j_0}=2$ curve in Fig. 4 are caused by resonances. Although these features are interesting, we have not attempted to analyze them in detail.

Figure 5 shows the orientationally averaged dissociation probabilities for the $j=0$, 3, and 4 states as a function of translational energy. For comparison purposes, the dissociation probability for H_2 in the ground vibrational state obtained from a functional fit to experimental data is shown

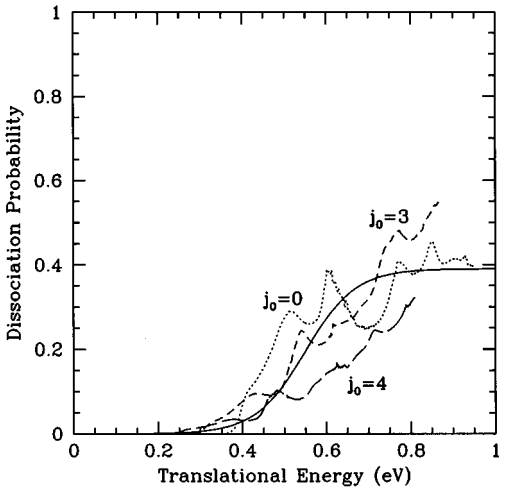

FIG. 5. Orientationally averaged dissociation probabilities for the $j_0=0$, 3, and 4 rotational states. A functional fit to the experimentally observed dissocation probability is shown (Ref. 57).

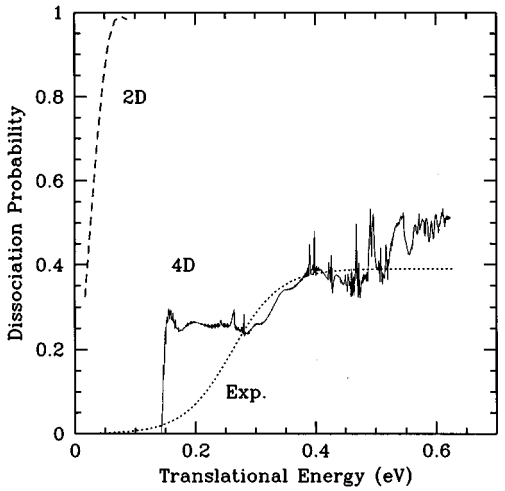

FIG. 6. Comparison of experimental and computed 2D and 4D dissociation probabilities for molecules in the $\nu_0=1$ state.

again.[57] It is difficult to specify particular values for the saturation values, width, and energetic thresholds of the computed curves for each j using the functional form given in Eq. (11). However, it is evident that the threshold energy increases with increasing j quantum number, indicating that for translational energies comparable to the barrier height, rotational energy hinders dissociation for the low j states examined here. The width of the dissociation curves increases with increasing j, also. Although detailed experimental results on the H_2/Cu(100) system are not available, these predictions are consistent with experimental results for H_2 on Cu(111),[9,10] which showed that rotation inhibits dissociation for $j<4$ and enhances it for higher j values. The widths of the experimental dissociation curves were found to broaden slightly (i.e., the slopes decreased) with increasing j but to a lesser extent than in the computed curves shown here.

Figure 5 indicates that the translational energy at which the dissociation probability becomes nonzero decreases for increasing j. The total energies (rovibrational+translational) at which the dissociation probabilities first become nonzero are nearly the same for the averaged states. However, the slope of the $j_0=0$ curve is the steepest, followed by that of the $j_0=3$ curve. This suggests that in low-energy collisions, rotational energy can couple to the reaction coordinate and be used to help cross the energetic barrier. However, the same amount of energy would be much more effective in promoting dissociation if it were put in translation.

Experimental observations indicate that vibrationally excited H_2 is responsible for most of the dissociation seen at low incident translational energies.[57] The results of calculations for H_2 initially in the $\nu_0=1$, $j_0=0$ state are shown in Fig. 6. The dissociation probability for vibrationally excited molecules obtained from a fit to experimental observations is shown, also.[57] The computed dynamical threshold is about 0.1 eV below the experimental value, roughly the same difference as was seen for dissociation from the ground state. The computed 4D curve is much narrower than the experimental curve but the saturation values of 0.5 (theory) and 0.39 (experiment) are in fairly good agreement. Comparing Figs. 2 and 6 shows that dissociation occurs at lower translational energies for vibrationally excited molecules than those in the ground state. This occurs because some of the energy initially in vibrational motion is converted to energy along the reaction path and can be used to cross the dissociation barrier in the products channel.[14–16] The fraction of the vibrational energy used to cross the barrier is quantified using the vibrational efficacy

$$\kappa=\frac{E_0(0)-E_0(1)}{E(\nu=1)-E(\nu=0)}, \tag{12}$$

where $E_0(\nu)$ is the dissociation threshold for the initial vibrational state ν and $E(\nu)$ is the energy of gas-phase H_2 in vibrational state ν. The values of $E_0(0)=0.47$ eV and $E_0(1)=0.15$ eV are determined from Figs. 2 and 6, respectively. These values are approximate because of the uncertainty in the saturation values and the amount of structure in the theoretical curve. The separation of the gas-phase $\nu=0$ and $\nu=1$ vibrational levels for the interaction potential used is 0.504 eV. This produces a value of $\kappa=0.64$, which is the same as that derived from the experiments.[57] Calculations for H_2/Cu(100) using a 4D model that included translation parallel to the surface but omitted rotational motion yielded $\kappa=0.75$.[38] For comparison purposes, the dissociation probability computed using a 2D model[18] with $\theta=90°$ and $\phi=0°$ are shown in Fig. 6. As was the case for the ground vibrational state, the dynamical threshold for the $\nu=1$ vibrational state is shifted to a lower energy and the saturation value is greater than for the 4D model. The vibrational efficacy computed from the 2D results is 0.48.

The curve in Fig. 6 that was computed using the 4D model shows a great deal of structure that can be attributed to resonances because of the rapid changes of phase of certain S-matrix elements as the energy changes. We have not attempted to analyze these features in detail. The wave func-

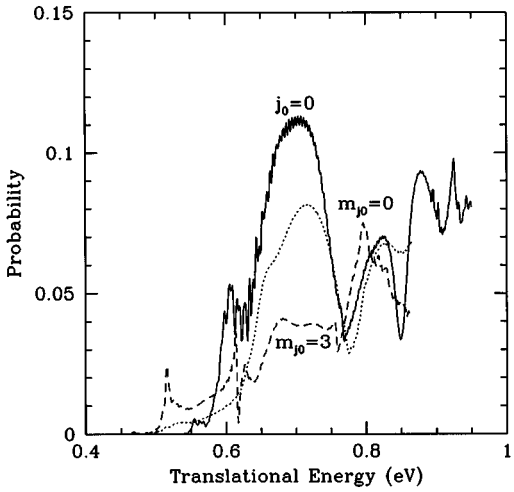

FIG. 7. Dependence of vibrational excitation probabilities on incident translational energy for H_2 incident in the $j_0=0$, ($j_0=3$, $m_{j_0}=0$), and ($j_0=3$, $m_{j_0}=3$) rotational states.

tion for this initial state was propagated for twice as long as those for the ground vibrational states. Small changes in the probabilities are still observed near the resonances, indicating some uncertainty in the details of the curves at these energies. However, the overall shape of the curve did not change significantly as the propagation time increased.

The final-state distribution of H_2 molecules that survive the collision with the surface and scatter back into the gas phase is of interest, also. Figure 7 shows the probabilities for vibrational excitation for H_2 incident in the $j_0=0$, ($j_0=3$, $m_{j_0}=0$), and ($j_0=3, m_{j_0}=3$) rotational states. The probabilities plotted are summed over all open rotational states of the $\nu=1$ final vibrational state. These curves indicate that the probabilities for vibrational excitation are significant. Although the $\nu=1$, $j=0$ channel is energetically open at $E_i=0.504$ eV for $j_0=0$, the probability for vibrational excitation does not become nonzero until $E_i=0.55$ eV. The probability eventually reaches a maximum of about 0.12. The probabilities for H_2 incident in the $j_0=3$ states are slightly lower in magnitude. The vibrational excitation probability is an order of magnitude greater than that predicted in our earlier 2D model for bridge-to-hollow dissociation using the same potential.[18] This indicates that rotational motion (i.e., allowing the molecule to sample orientations where $\theta\neq 90°$) has a strong effect on the dynamics of vibrational excitation. Experimental measurements of vibrational excitation probabilities on this system have yet to be made. However, large excitation probabilities were observed in the scattering of H_2 and D_2 from Cu(111).[7,59] Large probabilities of vibrational deexcitation ($\nu=1\rightarrow 0$) were observed for H_2 on Cu(110).[60] The results of these calculations are consistent with the behavior observed on these surfaces.

To better understand the reasons for the differences between the amount of vibrational elasticity predicted by the 2D and 4D models, a series of 2D calculations were performed in which the angles θ and ϕ were kept fixed at a number of different values. In the first calculations scattering

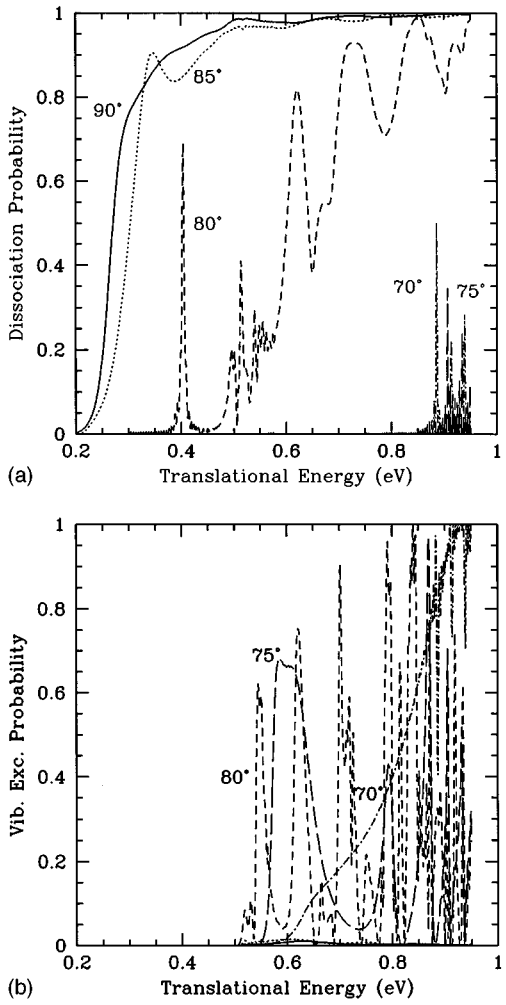

FIG. 8. Probabilities for (a) dissociation and (b) vibrational excitation for different orientations of the molecular bond in 2D calculations with $\phi=0°$.

with $\phi=0°$ (bridge-to-hollow) was examined for different values of θ. The probabilities for vibrational excitation and dissociation are shown in Fig. 8. Strictly speaking, dissociation should occur only for $\theta=90°$ in a 2D model since for tilted orientations at the surface the Pauli repulsion increases with increasing bond length because one of the H atoms moves down into the surface as the other moves away from the surface. Thus, even if sufficient energy is available to lengthen the bond near the surface initially, ultimately the PES becomes repulsive, the atoms recombine and scatter back into the gas phase. However, in the computational model used here, an optical potential absorbs the wave function when the bond length is extended beyond $4.8a_0$. The vibrational excitation and dissociation probabilities computed using the 2D model, therefore, depend on the location of the optical potential. Examination of the qualitative behavior of the 2D model lends insight into the results of the 4D model calculations, however. In the 4D calculations, dissociation can occur for slightly tilted orientations, although the barrier will be higher, since even after the barrier is crossed, the molecule can rotate into a lower energy conformation with $\theta=90°$. Figure 8(a) shows that within the 2D

model as θ decreases from 90° the dissociation threshold increases. This is understandable since the lowest dissociation barrier occurs for $\theta=90°$. For tilted orientations, the barrier is higher since the Pauli repulsion between the surface and the H atom nearest the surface increases to a greater extent than the repulsion between the surface and the other H atom decreases. The calculations indicate that even tilted molecules can cross the barrier and dissociate if sufficient energy is available. This is consistent with a picture of dissociation occurring for molecules oriented within a range of angles centered around $\theta=90°$.

Turning next to Fig. 8(b), we see that vibrational excitation is observed for translational energies greater than 0.504 eV, which is the excitation energy for this transition. Excitation probabilities for $\theta=90°$ and 85° are quite small for all energies examined with a maximum value of only 0.02. Figure 8(a) shows that the dissociation probabilities are near unity for these angles for energies greater than the excitation energy. Large vibrational excitation probabilities are seen for $\theta=80°$ and 75° near the energetic threshold and for $\theta=70°$ at higher energies. Although probabilities are not shown here, vibrational excitation is seen for values of θ down to 60°.

To explain the θ dependence of the vibrational excitation probability, the PES for bridge-to-hollow dissociation is shown for both $\theta=90°$ and $\theta=75°$ in Fig. 9. Tilting the molecule is seen to have two effects: (i) the barrier may become later or even disappear, the potential becoming purely repulsive for large r values, and (ii) due to the increased Pauli repulsion, the reaction path shows a greater degree of curvature as the molecule approaches the surface. Previous model calculations[56] have shown that a PES that effectively causes vibrational excitation shows essentially these two features. The high curvature in the reaction path provides the coupling necessary to excite the mode perpendicular to the reaction path. If the barrier is later (or if the potential along the reaction path is rather flat, though increasingly repulsive, with no barrier because there is no minimum at the products side), there will be more time for the coupling to effect the excitation before the barrier is reached (if there is a barrier present). This excitation may then result in reflection off the barrier or off the purely repulsive potential, and if the mode perpendicular to the reaction path is not deexcited during the descent of the reaction path, the molecule will emerge back to the gas phase in a vibrationally excited state.

In the second series of 2D calculations, collisions with $\phi=90°$ (bridge-to-top) for different values of θ were examined. The vibrational excitation probabilities for this orientation were significantly smaller than those for $\phi=0°$. The probabilities do not become nonzero until the translational energy nears 0.85 eV, reaching a maximum value of 0.17 at $E_i=0.94$ eV for $\theta=90°$. Note this is at the upper end of the energy range of the 4D results shown in Fig. 7. Dissociation probabilities for the 2D model with the bridge-to-top orientation were very small for all energies examined. Comparison of these results with those from the 2D bridge-to-hollow collisions indicates that the dissociation and vibrational excitation seen in the 4D calculations result primarily from collisions in which the molecular axis is oriented approximately toward the hollow sites.

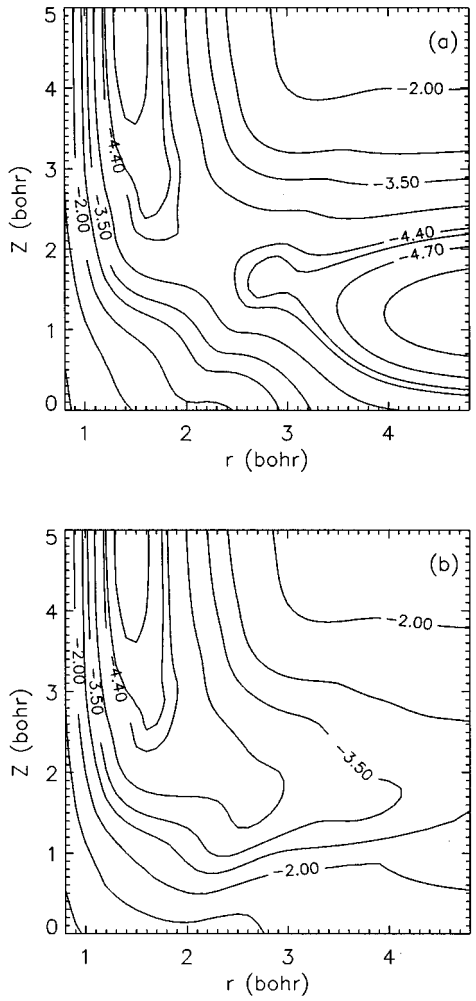

FIG. 9. Contour plots (labels in eV) are shown for the PES as a function of the molecule–surface distance, Z, and the H–H distance, r for (a) $\theta=90°$ and (b) $\theta=75°$.

Whether or not reaction and vibrational excitation occur in similar or in different regions of the PES has been the subject of some controversy. Observing similarities in the energy dependence of these two processes, Rettner *et al.*[7] first suggested that these processes should occur in similar regions of the PES. This idea was considered in subsequent dynamics calculations by Darling and Holloway[61] using a fixed-site 2D model. Within this model, using different model potentials, they were not able to reproduce the relative positions of the experimental values of the dynamical thresholds for reaction[57] and vibrational excitation[7] for H_2 scattering of Cu(111). From their results, they suggested that reaction and vibrational excitation should occur primarily on different surface sites. With the potentials they used (where vibrational excitation was efficient also for $\theta=90°$), no major difference was found in the relative positions of the thresholds when a rotational degree of freedom was added to the model.

Subsequently, the influence of parallel translational mo-

tion on vibrational excitation was considered by us,[37,38] employing a 4D model in which the orientation of the molecule was kept fixed at $\theta=90°$. Consistent with the suggestion of Darling and Holloway, vibrational excitation was found to occur almost exclusively in collisions near top sites, reaction being more efficient in collisions with the bridge and hollow sites. In our first paper,[37] we have argued that it should be possible to generalize our results to a model including rotations. This was done by considering the influence of collisions in which the molecular axis is almost perpendicular to the surface, which should lead to neither reaction nor vibrational excitation. However, we did not consider the possibility that collisions in which the molecular axis is tilted slightly out of the orientation parallel to the surface might produce very different results, as is here seen to be the case for collisions with the reactive bridge site.

While the present results clearly show that vibrational excitation may also occur in collisions with the reactive bridge site, we note that collisions with the top site may still be more effective in a model also considering the rotations (because collisions with $\theta=90°$ cause vibrational excitation also for this site, and it is likely that slightly tilted orientations will also be effective in causing vibrational excitation). Whether this is the case will be the topic of a future 6D study, which will also present results of fixed-site calculations for impacts on the top and hollows sites. We note that, even in the present 4D calculations, reaction and vibrational excitation occur most efficiently in different regions of the PES, in the sense that collisions with $\theta=90°$ are most effective in causing reaction, while collisions with slightly tilted orientations are most effective in causing vibrational excitation. However, the issue of where on the PES these two processes occur appears to be more subtle and less clear cut than suggested by previous studies.[7,37,38,61] In particular, vibrational excitation is here seen to occur also in collisions with the most reactive site.

Before considering rotational excitation, we briefly turn to the resonances that are clearly seen in the 2D calculations with θ fixed at values other than 90° [Figs. 8(a) and 8(b)], and also in the 4D calculations (e.g., Figs. 2 and 6). While it would be interesting to consider the physics responsible for the resonances, we have not done so in the present work. However, we wish to stress that the resonances should not result from the procedure used in fitting the potential. As was discussed in Ref. 39, due to the use of switching functions, the 2D potentials on which the 4D potential used in this work is based (see Sec. II) are not completely smooth. This can be seen in the functional dependence of the potential on the reaction path coordinate, which exhibits small features that are artifacts produced by the use of switching functions (see Fig. 6 of Ref. 39 and the accompanying discussion in that work). However, as discussed in Ref. 39, the ''size'' of the features is very small, as is the extent of coordinate space over which they occur (much smaller than the wavelength that may be associated with nuclear motion). For this reason, it is very unlikely that trapping in these features could cause the resonances seen in some of the figures presented in this work.

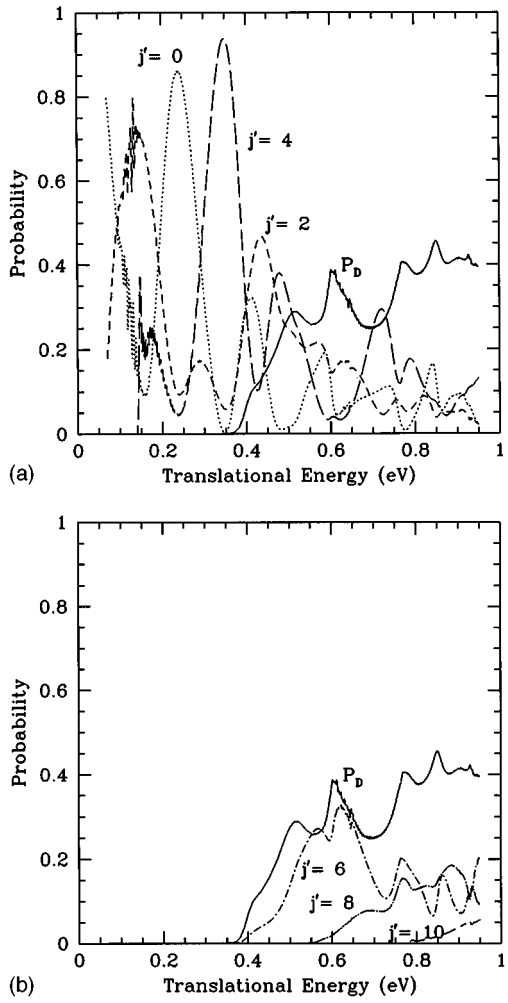

FIG. 10. Comparison of the translational energy dependence of the rotational transition and dissociation probabilities for (a) $j'=0$, 2, 4 and (b) $j'=6$, 8, 10.

Probabilities for rotational transitions into the gas-phase states $j'=0,2,4$ and $j'=6,8,10$ for $j_0=0$ are compared with the dissociation probability in Figs. 10(a) and 10(b), respectively. Probabilities for rotationally inelastic scattering can be quite large, reaching nearly unity, for energies below the dissociation threshold. Such large probabilities for rotational excitation of H_2 in low-energy scattering are not typical. Other computational models for dissociation predict significant rotational excitation only for energies at or above the dynamical threshold for dissociation.[20,28,30] Computational models for nonreactive scattering typically yield small probabilities for rotational excitation of H_2 at low collision energies.[41,62,63] Our results for rotational excitation are in broad agreement with recent measurements of high rotational excitation probabilities ($j=0\rightarrow2$) in scattering of D_2 from Cu(100) at low collision energies (<0.3 eV) at off-normal incidence.[64]

Rotationally inelastic scattering continues to be important as the dissociation channel opens up. Figure 10(b) indicates large probabilities for scattering into rotational states with large j quantum numbers for energies above the disso-

ciation threshold. Previous computational studies report significant rotational inelasticity accompanying dissociation, but the reported populations of scattered molecules in high j levels are smaller than those predicted here.[30] Rotational excitation accompanying dissociation has previously been explained using a ''gap'' model,[65] which considered an incident wave function representing an isotropic rotational distribution of molecules. As the wave function reaches the surface, the contribution representing molecules lying parallel to the surface dissociates. The remaining portion of the wave function scatters back into the gas phase and is found to have a significant population of rotationally excited states when projected onto rotor states. The high rotational inelasticity seen here for energies below the dissociation threshold and large populations seen for high j states that accompany dissociation suggest that ''mechanical'' excitation due to strong rotational anisotropy of the potential is also playing an important role here.

The H_2 molecules scattered back into the gas phase can be analyzed in terms of their rotational alignment, which describes the distribution of the orientation of the rotational angular momentum vector. Following Corey and Alexander,[66] the quadrupole moment, $A_{j'}^2$, is computed as

$$A_{j'}^2(E') = \frac{5(-1)^{2-j'}\Sigma_{m_j'}(-1)^{m_j'}\begin{pmatrix} j' & j' & 2 \\ -m_j' & m_j' & 0 \end{pmatrix}|S_{000\to j'm_j'\nu'}(E')|^2}{(2j'+1)^{-1/2}\Sigma_{m_j'}|S_{000\to j'm_j'\nu'}(E')|^2}. \tag{13}$$

If $A_{j'}^2 = 0$, the m_j' values are distributed in an isotropic fashion. If $A_{j'}^2 = -2.5$, the molecules are predominately rotating in a plane perpendicular to the surface with a cartwheel-type motion and $m_j' = 0$. Similarly, if $A_{j'}^2 = 5$ the molecules are aligned with $m_j' = j'$ and the rotation will be as nearly in the plane of the surface as possible in a helicopter-type motion. Figure 11 shows the quadrupole moment for two different final rotational states as a function of incident translational energy. The incident molecules were in the ground rovibrational state. The polarization of the reflected molecules is strongly dependent on the translational energy. For example, at the lowest energies shown, the scattered $j'=2$ molecules are rotating primarily in a cartwheel manner ($\Delta m_j = 0$). As the energy increases, the distribution becomes isotropic and then is heavily weighted toward helicopter-type motion for $E'=0.27$ eV. Further oscillations are seen as the energy continues to increase. The energy dependence of the polarization of the $j'=4$ state is similar to that of the $j'=2$ state.

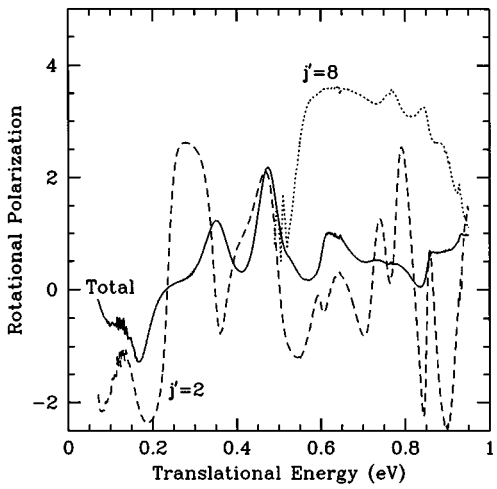

FIG. 11. Polarization ratio for final rotational states j' as a function of incident translational energy.

The polarization of the $j'=8$ rotational state, which is representative of states that are populated only for energies above the dissociation threshold, is qualitatively different. In particular, $A_{j'}^2$ is greater than zero for $j'=8$ for all incident energies shown in Fig. 11. Molecules scattered into the $j'=6$, 8, and 10 states tend to come off the surface with their angular momentum vector pointing more toward the surface normal, i.e., with helicopterlike rotation.

Figure 11 also shows the total polarization of scattered H_2 molecules, computed by including summations over j' in the numerator and denominator of Eq. (13). The total polarization is negative only for energies less than 0.25 eV. The total polarization for low energies is less negative than that of the $j'=2$ state because of the significant fraction of molecules that are scattered elastically into the $j'=0$ state; these molecules are, by definition unpolarized. At higher collision energies, there is a preference for molecules to scatter from the surface as helicopters rather than cartwheels. However, the distribution is close to isotropic for most of the energy range above the dynamic threshold. In contrast, the gap model as applied to flat surfaces predicts that the scattered molecules should rotate in a cartwheel fashion. This suggests that the gap model should be modified for the case where the PES is also strongly corrugated in ϕ, but it also suggests that ''mechanical'' rotational excitation (caused simply by the anisotropy of the PES) is very important here.

IV. CONCLUSIONS

Results have been presented of quantum dynamical calculations on the reaction of H_2 on Cu(100), employing a 4D fixed-site model in which the impact site is fixed to the surface bridge site. The model allows one to investigate the influence of the rotations of the molecule on the dissociation dynamics in a qualitative fashion. The PES used came from

density functional calculations that were performed within the generalized gradient approximation, using a slab representation of the surface.

The computed dissociation probabilities are in reasonable agreement with curves obtained from an analysis of experimental measurements. The saturation values and vibrational efficacy are in good agreement with the experiment but the computed dynamical thresholds are too low by about 0.1 eV. Also, the computed dissociation curve for H_2 in the ground rovibrational state is narrower. These differences arise, in part, from neglect of translational motion parallel to the surface. In a 6D calculation the effective barrier height should increase because of the additional zero-point energy associated with motion in X and Y. The variation of the barrier height with the impact site should broaden the computed curve, which should have the effect of pushing the dynamical threshold up further. Another possible source of the disagreement is in the PES, but we note that the present 4D result (a dynamical threshold which is *too low* by 0.1 eV) is not unexpected. A more conclusive verdict on the accuracy of the PES can only be given in 6D calculations, which we hope to perform in the near future.

Large probabilities for vibrational excitation are predicted, similar in magnitude to those seen in experiments on scattering from other copper surfaces. The calculations indicate that vibrational excitation and dissociation can occur at the same site, though with different efficiencies for differing orientations. In particular, reaction is most efficient for $\theta=90°$, while vibrational excitation occurs most efficiently for tilted orientations. Calculations using a 4D model treating translational motion parallel to the surface, but omitting rotation, predicted similar probabilities for vibrational excitation but suggested that vibrational excitation should occur almost exclusively in collisions with top sites while reaction should be more efficient above the bridge and hollow sites. The new results show that the issue of where on the PES vibrational excitation and reaction occur is more subtle, in that vibrational excitation is here seen to be effective also in collisions with the most reactive site.

Large probabilities for rotationally inelastic scattering accompany dissociation. The rotational inelasticity may be substantial, leading even to the population of the $j=8$ and $j=10$ states. Molecules excited to high j states rotate predominantly with helicopter-type motion. The high level of rotational inelasticity is caused at least in part by the strong anisotropy in θ and ϕ of the potential.

The dynamical threshold for dissociation shifts to higher translational energies as the j_0 rotational quantum number of the incident H_2 increases. State-resolved experimental dissociation probabilities are not available for the Cu(100) surface but this behavior is observed also for Cu(111) for low j. The model predicts that dissociation probabilities for molecules with helicoptering and cartwheel rotational motions are comparable. This is consistent with the experimental observation of an isotropic distribution of D_2 associatively desorbed from Cu(111), but inconsistent with results of earlier calculations that predicted much larger reaction probabilities for the helicopter rotation. Although the detailed experimental measurements needed to confirm many of these predictions are not always available for the Cu(100) surface, it is encouraging that the predictions are in qualitative agreement with experiments on other Cu surfaces, where available. Nevertheless, confirmation of many of the predictions presented here will require additional experimental measurements on the H_2+Cu(100) system and we hope that such experiments will be performed.

ACKNOWLEDGMENTS

The work at NRL was supported by the Office of Naval Research through the Naval Research Laboratory. This work was supported in part by a grant of HPC time from the DoD HPC Shared Resource Center, U.S. Army Corp of Engineers Waterway Experiment Station Cray C-90. The research of one of the authors (G.J.K) was supported by the Royal Netherlands Academy of Arts and Sciences and by a grant of computer time by the Dutch National Computing Facilities Foundation (NCF). This work was also supported by the Netherlands Foundation for Chemical research (SON) with financial aid from the Netherlands Organization for Scientific Research (NWO).

[1] B. E. Hayden and C. L. A. Lamont, Phys. Rev. Lett. **63**, 1823 (1989).
[2] H. F. Berger, M. Leisch, A. Winkler, and K. D. Rendulic, Chem. Phys. Lett. **175**, 425 (1990).
[3] B. E. Hayden and C. L. A. Lamont, Surf. Sci. **243**, 31 (1991).
[4] A. Hodgson, J. Moryl, and H. Zhao, Chem. Phys. Lett. **182**, 152 (1991).
[5] D. J. Auerbach, C. T. Rettner, and H. A. Michelsen, Surf. Sci. **283**, 1 (1993).
[6] C. T. Rettner, D. J. Auerbach, and H. A. Michelsen, Phys. Rev. Lett. **68**, 1164 (1992).
[7] C. T. Rettner, D. J. Auerbach, and H. A. Michelsen, Phys. Rev. Lett. **68**, 2547 (1992).
[8] C. T. Rettner, H. A. Michelsen, and D. J. Auerbach, Faraday Discuss. **96**, 17 (1993).
[9] H. A. Michelsen, C. T. Rettner, D. J. Auerbach, and R. N. Zare, J. Chem. Phys. **98**, 8294 (1993).
[10] C. T. Rettner, H. A. Michelsen, and D. J. Auerbach, J. Chem. Phys. **102**, 4625 (1995).
[11] M. Balooch, M. J. Cardillo, D. R. Miller, and R. E. Stickney, Surf. Sci. **46**, 358 (1974).
[12] G. Anger, A. Winkler, and K. D. Rendulic, Surf. Sci. **220**, 1 (1989).
[13] P. B. Rasmussen, P. M. Holmblad, H. Christoffersen, P. A. Taylor, and I. Chorkendorff, Surf. Sci. **287/288**, 79 (1993).
[14] M. Hand and S. Holloway, Surf. Sci. **211/212**, 940 (1989).
[15] J. Harris, Surf. Sci. **221**, 335 (1989).
[16] M. R. Hand and S. Holloway, J. Chem. Phys. **91**, 7209 (1989).
[17] D. Halstead and S. Holloway, J. Chem. Phys. **93**, 2859 (1990).
[18] G. Wiesenekker, G. J. Kroes, E. J. Baerends, and R. C. Mowrey, J. Chem. Phys. **102**, 3873 (1995); **103**, 5168 (1995).
[19] S. Holloway, J. Phys. Condens. Mater. **3**, S43 (1991).
[20] U. Nielsen, D. Halstead, S. Holloway, and J. K. Norskov, J. Chem. Phys. **93**, 2879 (1990).
[21] A. J. Cruz and B. Jackson, J. Chem. Phys. **94**, 5715 (1991).
[22] J. Sheng and J. Z. H. Zhang, J. Chem. Phys. **96**, 3866 (1992).
[23] J. Sheng and J. Z. H. Zhang, J. Chem. Phys. **97**, 6784 (1992).
[24] P. Saalfrank and W. H. Miller, J. Chem. Phys. **98**, 9040 (1993).
[25] J. Sheng and J. Z. H. Zhang, J. Chem. Phys. **99**, 1373 (1993).
[26] R. C. Mowrey, J. Chem. Phys. **99**, 7049 (1993).
[27] J. Dai, J. Sheng, and J. Z. H. Zhang, J. Chem. Phys. **101**, 1555 (1994).
[28] G. R. Darling and S. Holloway, J. Chem. Phys. **101**, 3268 (1994).
[29] J. Dai and J. Z. H. Zhang, Surf. Sci. **319**, 193 (1994).
[30] J. Dai and J. Z. H. Zhang, J. Chem. Phys. **102**, 6280 (1995).
[31] D. Halstead and S. Holloway, J. Chem. Phys. **88**, 7197 (1988).

[32] G. R. Darling and S. Holloway, Chem. Phys. Lett. **191**, 396 (1992).
[33] G. R. Darling and S. Holloway, J. Chem. Phys. **97**, 5182 (1992).
[34] G. R. Darling and S. Holloway, Surf. Sci. **304**, L461 (1994).
[35] A. Gross, J. Chem. Phys. **102**, 5045 (1995).
[36] A. Gross, B. Hammer, M. Scheffler, and W. Brenig, Phys. Rev. Lett. **73**, 3121 (1994).
[37] G. J. Kroes, G. Wiesenekker, E. J. Baerends, and R. C. Mowrey, Phys. Rev. B **53**, 10 397 (1996).
[38] G. J. Kroes, G. Wiesenekker, E. J. Baerends, and R. C. Mowrey, J. Chem. Phys. **105**, 5979 (1996).
[39] G. Wiesenekker, G. J. Kroes, and E. J. Baerends, J. Chem. Phys. **104**, 7344 (1996).
[40] R. C. Mowrey and D. J. Kouri, Chem. Phys. Lett. **119**, 285 (1985).
[41] R. C. Mowrey and D. J. Kouri, J. Chem. Phys. **84**, 6466 (1986).
[42] D. J. Kouri and R. C. Mowrey, J. Chem. Phys. **86**, 2087 (1987).
[43] G. J. Kroes, J. G. Snijders, and R. C. Mowrey, J. Chem. Phys. **102**, 5512 (1995).
[44] G. J. Kroes, J. G. Snijders, and R. C. Mowrey, J. Chem. Phys. **103**, 5121 (1995).
[45] R. C. Mowrey, J. Chem. Phys. **94**, 7098 (1991).
[46] H. Tal-Ezer and R. Kosloff, J. Chem. Phys. **81**, 3967 (1984).
[47] M. D. Feit, J. A. Fleck, Jr., and A. Steiger, J. Comput. Phys. **47**, 412 (1982).
[48] D. Kosloff and R. Kosloff, J. Comput. Phys. **52**, 35 (1983).
[49] G. G. Balint-Kurti, R. N. Dixon, and C. C. Marston, J. Chem. Soc. Faraday Trans. **86**, 1741 (1990).
[50] C. C. Marston, G. G. Balint-Kurti, and R. N. Dixon, Theor. Chim. Acta **79**, 313 (1991).
[51] G. G. Balint-Kurti, R. N. Dixon, and C. C. Marston, Int. Rev. Phys. Chem. **11**, 317 (1992).
[52] R. C. Mowrey and G. J. Kroes, J. Chem. Phys. **103**, 1216 (1995).
[53] T. Seideman and W. H. Miller, J. Chem. Phys. **96**, 4412 (1992).
[54] A. Gross, S. Wilke, and M. Scheffler, Phys. Rev. Lett. **75**, 2719 (1995).
[55] A. D. Kinnersley, G. R. Darling, S. Holloway, and B. Hammer, Surf. Sci. **364**, 219 (1996).
[56] G. R. Darling and S. Holloway, J. Chem. Phys. **97**, 734 (1992).
[57] H. A. Michelsen and D. J. Auerbach, J. Chem. Phys. **94**, 7502 (1991).
[58] D. Wetzig, M. Rutkowski, R. David, and H. Zacharias, Europhys. Lett. **36**, 31 (1996).
[59] A. Hodgson, J. Moryl, P. Traversaro, and H. Zhao, Nature **356**, 501 (1992).
[60] M. Gostein H. Parhikhteh, and G. O. Sitz, Phys. Rev. Lett. **75**, 342 (1995).
[61] G. R. Darling and S. Holloway, Surf. Sci. **307–309**, 153 (1994).
[62] G. J. Kroes and R. C. Mowrey, Chem. Phys. Lett. **232**, 258 (1995).
[63] G. J. Kroes and R. C. Mowrey, J. Chem. Phys. **103**, 2186 (1995).
[64] M. Bertino (private communication).
[65] S. Holloway and B. Jackson, Chem. Phys. Lett. **172**, 40 (1990).
[66] G. C. Corey and M. A. Alexander, J. Chem. Phys. **87**, 4937 (1987).